STM JOURNALS

Journal of
Polymer & Composites
https://journals.stmjournals.com/jopc

ISSN: 2321-2810 (Online)
ISSN: 2321-8525 (Print)
Volume 14, Special Issue 1, 2026
DOI (Journal): 10.37591/JoPC

Research JoPC

Optimizing Parameters for Dry Sliding Wear Control in Stir-Cast AA7050/SiC Composites

Varshitha Kothapalli[1], Ramatenki Chinna[2,*], Sireesha Koneru[3], V. Viswanath Shenoi[4], Boggarapu Nageswara Rao[5]

Abstract

Using a pin-on-disc tribometer, this study examined the dry sliding wear behavior of AA7050/SiC composites. The production of this metal matrix composite was achieved through the stir-casting process, which involved an initial step of melting the AA7050 alloy, followed by the careful introduction of silicon carbide (SiC) particles, stirring to achieve uniform dispersion, and finally, casting the molten mixture. Wear rate (WR) was determined by three operational parameters: SiC reinforcement content (A: 0, 4, 6 wt%), sliding velocity (B: 1, 2, 3 m/s), and sliding distance (C: 1000, 1400, 1800 m). The experimental design followed a Taguchi L_9 orthogonal array, conducting nine test runs. Statistical analysis, including a natural logarithm transformation of WR (lnWR) due to significant variation, determined parameter contributions. Results indicated that SiC reinforcement (A) and sliding distance (C) significantly influenced lnWR, while sliding velocity (B) had the least impact. An empirical relationship for WR was established and validated against measured data. The optimal parameters, determined by a modified Taguchi method, were A_3 (6% reinforcement), B_2 (2 m/s sliding velocity), and C_3 (1800 m sliding distance), yielding a minimum WR estimated to be in the range of 0.00175 to 0.00186 mm^3/m. Measured WR values confirmed this estimated range. To visually underscore the attainment of the low wear rate, WR curves were generated using the developed empirical relationship, specifically by fixing two process parameters at their optimal values, while progressively varying the third.

***Author for Correspondence**
Ramatenki Chinna

[1]B. Tech Student, Department of Computer Science Engineering, Koneru Lakshmaiah Education Foundation (KLEF), Deemed to be University, Green Fields, Vaddeswaram, Guntur, Andhra Pradesh, India
[2]Research Scholar, Department of Mechanical Engineering, Koneru Lakshmaiah Education Foundation (KLEF), Deemed to be University, Green Fields, Vaddeswaram, Guntur, Andhra Pradesh, India
[3]Assistant Professor, Department of Mechanical Engineering, Koneru Lakshmaiah Education Foundation (KLEF), Deemed to be University, Green Fields, Vaddeswaram, Guntur, Andhra Pradesh, India
[4]Professor & Head, Department of Integrated Research and Discovery, Koneru Lakshmaiah Education Foundation (KLEF), Deemed to be University, Green Fields, Vaddeswaram, Guntur, Andhra Pradesh, India
[5]Professor, Department of Integrated Research and Discovery, Koneru Lakshmaiah Education Foundation (KLEF), Deemed to be University, Green Fields, Vaddeswaram, Guntur, Andhra Pradesh, India

Received Date: 08 October 2025
Accepted Date: 27 October 2025
Published Date: 05 March 2026

Citation Varshitha Kothapalli, Ramatenki Chinna, Sireesha Koneru, V. Viswanath Shenoi, Boggarapu Nageswara Rao. Optimizing Parameters for Dry Sliding Wear Control in Stir-Cast AA7050/SiC Composites. Journal of Polymer & Composites. 2026; 14(Special Issue 1): S1624–S1635p.

Keywords: Metal matrix composite, Modified Taguchi Method, Operational parameters, Orthogonal Array, Pin-on-Disc, Wear Rate

INTRODUCTION

AA7050/SiC composites, made from AA7050 aluminum alloy and silicon carbide (SiC) particle reinforcement, see widespread use due to their thermal stability, high strength, and wear resistance [1-3]. Table 1(a) details the diverse industrial applications of this metal matrix composite (MMC) [2-8].

In contrast to monolithic AA7050 alloy, AA7050/SiC composites typically display improved wear resistance, which is mainly due to the reinforcing impact of SiC particles. Factors such as temperature, applied load, sliding speed, and the Mechanically Mixed Layer (MML) development influence the wear characteristics of MMCs [1-4, 9]. Table 1(b) provides information on the fabrication methods of this MMC [1, 3, 10-13], and Table 1(c) summarizes key findings related to its wear resistance [2, 3, 14-23]. Future research focuses on optimizing composite performance through the investigation of SiC particle size, shape, and distribution variations, alongside the exploration of novel manufacturing techniques.

The dry sliding wear of stir-cast AA7050/SiC composites using a pin-on-disc setup shown in Figure 1.[24]. Their experimental design employed Taguchi's L9 orthogonal array (OA) to evaluate three input variables—% reinforcement of SiC, sliding velocity, and sliding distance—each at three distinct levels. They concluded that sliding distance had significant impact on wear, while sliding velocity had only a minimal effect.

This article extends prior research by proposing an empirical equation to model wear rate (WR) from operational parameters, subsequently validating it with measured data. This empirical model facilitates the generation of output responses for a full factorial experimental design, enabling the identification of an optimal solution. The optimal parameters were directly ascertained from the ANOVA (Analysis of Variance) results, which were derived from the measured WR data obtained via Taguchi's L9 OA. The identified optimal operational parameters resulted in the lowest WR, a finding estimated using a modified Taguchi method and corroborated by observed values. A concise overview of this analysis is provided hereafter.

Table 1. (a) Industrial Applications of AA7050/SiC Composites [2-8]

Application Area	**Components**	**Benefits**
Aerospace Industry [2, 4]	Fuselage structures, Landing gear parts	High strength and fatigue resistance
Automotive Sectors [2, 3, 5]	Engine components, Suspension systems, Chassis parts	High strength, wear resistance, and thermal stability
Defence Industry [2, 3]	Military vehicles, Weaponry, Protective equipment	Enhanced strength and durability
Sports Equipment [6-8]	Bicycle frames, Golf clubs	Better handling and safety
Industrial Machinery [2]	Bearings, Gears	Enhanced wear resistance and strength

Table 1. (b) Methods used to fabricate AA7050/SiC composites [1, 3, 10-13]

Method	**Description**
Stir Casting [3, 10]	A cost-effective method for mass production, it disperses SiC particles into molten AA7050 alloy.
Powder Metallurgy [3, 11]	This technique blends AA7050 powder with SiC particles, followed by compaction and sintering.
Friction Stir Processing (FSP) [1, 12, 13]	This process involves a rotating tool for localized heat generation and mechanical mixing of AA7050 and SiC, culminating in a refined microstructure

Table 1. (c) Key findings on AA7050/SiC Composite Wear Resistance [2, 3, 14-23]

Influence	**Wear Resistance of MMC**
SiC Reinforcement [2, 3, 14]	Reinforcing AA7050 with SiC particles significantly improves wear resistance, owing to the hardness and strength these ceramic particles impart
Temperature [3, 14]	Wear rate generally increases with temperature, particularly beyond a certain threshold (e.g., 200°C), due to alterations in the MML and changes in material properties
Sliding Speed [15, 16]	Wear rate can increase with sliding speed, although some research indicates a plateau within specific ranges
Applied Load [16, 17]	Higher applied loads typically result in increased wear due to greater deformation and friction
Mechanically Mixed Layer (MML) [3]	The initial formation of an MML on the worn surface can enhance wear resistance by serving as a protective layer. However, its degradation under high temperatures or severe conditions can shift the wear mechanism to more aggressive modes
Particle Characteristics [2, 3,18]	The size, type, and distribution of SiC particles within the MMC.
Others [3, 19-23]	Subsequent heat treatment and the manufacturing processes.

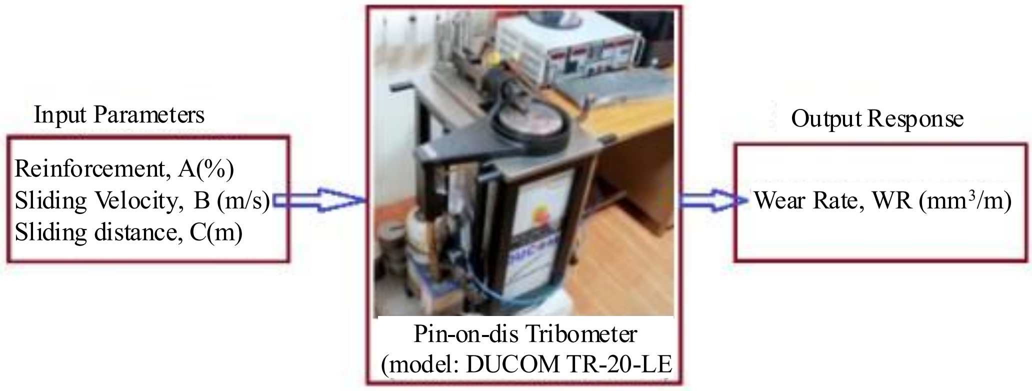

Figure 1. The experimental setup to study the wear characteristics of MMCs [24].

MATERIALS AND METHODS

Studies are made on the dry sliding wear of stir-cast AA7050/SiC composites using a DUCOM TR-20-LE pin-on-disc tribometer (See Figure 1) [24]. The composites were fabricated by stir-casting, a process that entailed melting AA7050 alloy, incorporating SiC particles, stirring for uniform dispersion, and casting. The AA7050 alloy primarily consists of 89% Al, 2.3% Cu, 2.3% Mg, 6.2% Zn, and 0.12% Zr. SiC properties noted were: 40.096 g•mol^{-1} molar mass, 3.16 g•cm^{-3} density, 2830°C melting point, approximately 900 cm^2/V•s electron mobility, -12.8 x 10^{-6} cm^3•mol^{-1} magnetic susceptibility, and 2.55 refractive index. Microscopic analysis verified the homogeneous SiC particle distribution.

Wear tests subsequently assessed composite performance. Test samples (9 mm diameter, 35 mm length) were prepared by cleaning with an emery sheet and kerosene immersion. Wear loss was calculated from pre- and post-test specimen weights. The wear rate (WR, mm^3/m) was determined at a constant 20 N load, while varying three parameters: SiC reinforcement (0, 4, 6%), sliding velocity (1, 2, 3 m/s), and sliding distance (1000, 1400, 1800 m).

To streamline experiments, Taguchi's L_9 Orthogonal Array (OA) was chosen. For this array, each input parameter from Table 2 was assigned three levels, and the OA subsequently defined the input parameters for each test run [25]. For three levels $(n_l = 3)$, the number of input parameters (n_p) according to Taguchi's L_9 OA is determined from [25].

$$N_{Tag} = 1 + n_P(n_l - 1) \Rightarrow n_P = \frac{(N_{Tag} - 1)}{(n_l - 1)} = \frac{(9-1)}{(3-1)} = \frac{8}{2} = 4 \tag{1}$$

In total, the L_9 design allows for nine tests $(N_{Tag} = 9)$, accommodating four input parameters. In this study, three parameters (*A*, *B*, and *C*) were selected, while an additional fictitious parameter, '*D*,' was added in Table 2, following the methodology proposed in references [26, 27]. The data recorded from the machining process for the nine sets of input parameters is presented in Table 3. Due to appreciable variation of *WR* in the nine test runs, the data is transformed to natural logarithm scale and designated the output response as $\ln WR$. A variance analysis (ANOVA) was conducted on the $\ln WR$ data from Table 3 and displayed the results in Table 4.

Table 2. Levels for the process parameters

Process parameters	Designation	1st level	2nd level	3rd level
SiC reinforcement (%)	*A*	0	4	6
Sliding velocity (m/s)	*B*	1	2	3
Sliding distance (m)	*C*	1000	1400	1800
Fictitious	*D*	D_1	D_2	D_3

Table 3. Wear rate, WR (mm^3/m) as per the Taguchi's L_9 OA.

Test Run	Process parameter levels				Wear rate, WR (mm^3/m)	$\ln WR = \ln(WR)$
	A	*B*	*C*	*D*		
1	1	1	1	1	0.00496	-5.3063
2	1	2	2	2	0.00387	-5.5545
3	1	3	3	3	0.00312	-5.7699
4	2	1	2	3	0.00358	-5.6324
5	2	2	3	1	0.00239	-6.0365
6	2	3	1	2	0.00412	-5.4919
7	3	1	3	2	0.00198	-6.2247
8	3	2	1	3	0.00273	-5.9035
9	3	3	2	1	0.00306	-5.7893

Table 4. ANOVA results indicating the significance of process parameters on $\ln WR$, whose grand mean value is -5.7454.

Process parameters	1st Mean	2nd Mean	3rd Mean	SOS (Sum of Squares)	%Contribution
A	-5.5436	-5.7203	-5.9725	0.2788	43.01
B	-5.7211	-5.8315	-5.6837	0.0354	5.46
C	-5.5672	-5.6587	-6.0104	0.3284	50.66
D	-5.7107	-5.7570	-5.7686	0.0056	0.87

Complex engineering optimization problems often involve unknown parameters that can introduce variability in output responses. While Taguchi's L_9 orthogonal array design accommodates four parameters at three levels, the current situation involved only three. To account for potential unmeasured influences, a fictitious fourth parameter (*D*) was introduced, and an ANOVA was conducted to assess its contribution. Parameter *D* represents either an unknown influencing factor or an error parameter in the measurements affecting the output response. As detailed in Table 4, reinforcement (*A*) and sliding distance (*C*) were found to significantly impact the overall mean value of $\ln WR$, contributing 43.01% and 50.66% respectively. In contrast, sliding velocity (*B*) and the fictitious parameter (*D*) contributed considerably less, at 5.46% and 0.87% respectively. The collective contribution of *A*, *B*, *C*, and *D* total 100%.

For the specified levels of *A*, *B*, and *C*, the output response $\ln WR$ is estimated employing the additive law [25] and using the data of ANOVA Table 4 from

$$\ln WR^e = \ln WR_g^m + \sum_{i=1}^{n_P}\left(\ln WR_{il}^m - \ln WR_g^m\right) = \sum_{i=1}^{n_P} \ln WR_{il}^m - (n_P - 1)\ln WR_g^m \tag{2}$$

Here, $\ln WR^e$ represents the estimated value of $\ln WR$;

$\ln WR_g^m = -5.7454$, is the grand mean of $\ln WR$; and

$\ln WR_{il}^m$ is the mean value of $\ln WR$ in ANOVA Table 4.

Subscript $'i'(i = 1,2,3)$ signifies the input parameters (*A*, *B*, *C*). Subscript $'l'(l = 1,2,3)$

signifies the 1st, 2nd, 3rd mean values of the $\ln WR$ to the parameter levels. For example,

Journal of Polymer & Composites
Volume 14, Special Issue 1
ISSN: 2321-2810 (Online), ISSN: 2321-8525 (Print)

$\ln W\,R_{22}^{m} = -5.8315$ corresponds to the 2nd mean value of $\ln WR$ for B in ANOVA table 4.

To demonstrate the simplicity of the present analysis, $\ln WR$ estimates in Test Run-1 (Table 5) are presented. For Test Run-1, the levels of (*A*, *B*, *C*, *D*) were set to (1, 1, 1, 1). The corresponding mean $\ln WR$ values extracted from ANOVA table 4 are: $ln\,W\,R_{11}^{m}$ =-5.5436; $ln\,W\,R_{21}^{m}$ =-5.7211; $ln\,W\,R_{31}^{m}$ =-5.5672; and $ln\,W\,R_{41}^{m}$ =-5.7107. The grand mean, $ln\,W\,R_{g}^{m} = -5.7454$.

In Test Run-1, using Eq. (2) excluding $D(n_P = 3)$, $\ln WR$ estimate:

$$ln\,W\,R^{e} = ln\,W\,R_{11}^{m} + ln\,W\,R_{21}^{m} + ln\,W\,R_{31}^{m} - 2 \times ln\,W\,R_{g}^{m}$$
$$= -5.5436 - 5.7211 - 5.5672 - 2 \times (-5.7454) = -5.3410$$

In Test Run-1, using Eq. (2) including $D(n_P = 4)$, $\ln WR$ estimate:

$ln\,W\,R^{e} = ln\,W\,R_{11}^{m} + ln\,W\,R_{21}^{m} + ln\,W\,R_{31}^{m} + ln\,W\,R_{41}^{m} - 3 \times ln\,W\,R_{g}^{m} = -5.5436 - 5.7211 - 5.5672 - 5.7107 - 3 \times (-5.7454) = -5.3063$The corrections to the estimates of $\ln WR$ for $n_P = 3$ obtained from the minimum and maximum deviation of mean values of D from the grand mean:

$$\min\{\ln WR_{41}^{m}, \ln WR_{42}^{m}, \ln WR_{43}^{m}\} - \ln WR_{g}^{m} = \min\{-5.7107, -5.7570, -5.7686\} - (-5.7454)$$
$$= -5.7686 + 5.7454 = -0.0232$$

$$\max\{\ln WR_{41}^{m}, \ln WR_{42}^{m}, \ln WR_{43}^{m}\} - \ln WR_{g}^{m} = \max\{-5.7107, -5.7570, -5.7686\} - (-5.7454)$$
$$= -5.7107 + 5.7454 = 0.0347$$

Applying these corrections to the estimate of $\ln WR$ with exclusion of *D*, the minimum and maximum estimates of $\ln WR$ obtained for Test Run-1 are -5.3642 (=-5.3410-0.0232) and -5.3063 (=-5.3410+0.0347).

For the specified levels of (*A*, *B* and *C*) in Taguchi L_9 OA, $\ln WR$ is evaluated using additive law (2). The lower and upper limits of $\ln WR$ in Table 5 are obtained after applying the corrections. Test data [24] is found to be within the estimated range. The additive law (2) can be used to estimate $\ln WR$ for the 27 combinations of three levels of three process parameters: $\left(\left(\left((A_i, B_j, C_k), k = 1to3\right), j = 1to3\right), i = 1to3\right)$ in which subscripts to parameters (*A*, *B*, *C*) are the levels. For this full factorial design of experiments, the sequence numbers are allotted from 1 to 27. The sequence numbers to the sets of input parameters for the 1 to 9 Test Runs in Taguchi's L_9 OA are 1, 5, 9, 11, 15, 16, 21, 22, and 26. Using Eq. (2), $\ln WR$ values were calculated for the framed 27 sets of input parameters. Test data in Figure 2 falls within the estimated limits.

After transforming the three levels of each parameter to coded values (-1, 0, and 1), the mean values of $\ln WR$ in ANOVA Table 4 are modeled with a quadratic polynomial. This quadratic model is then be integrated into the additive law (2) to obtain an empirical relationship for $\ln WR$ with input variables (*A*, *B*, *C*). The transformed process parameters are: $\xi_1 = \frac{1}{24}(A-4)(A+6)$; $\xi_2 = B - 2$; and $\xi_3 = \frac{1}{400}(C - 1400)$. From the mean values of $\ln WR$ (ANOVA table 4) and using the additive law (2), the empirical relationship developed is

$$\ln W\,R = -5.7197 - 0.21445\xi_1 - 0.03775\xi_1^2 + 0.0187\xi_2 + 0.1291\xi_2^2 - 0.2216\xi_3 - 0.1301\xi_3^2 \quad (3)$$

Table 5. Estimates of $\ln WR$.

Test Run	Machining parameters				Test [24]	Estimate Eq. (2)			Estimated range	
	A	*B*	*C*	*D*		$n_p = 3$	*R.E (%)*	$n_p = 4$	*Minimum*	*Maximum*
1	1	1	1	1	-5.3063	-5.341	-0.65	-5.3063	-5.3642	-5.3063
2	1	2	2	2	-5.5545	-5.5429	0.21	-5.5545	-5.5661	-5.5082
3	1	3	3	3	-5.7699	-5.7468	0.40	-5.7699	-5.7699	-5.7120
4	2	1	2	3	-5.6324	-5.6092	0.41	-5.6324	-5.6324	-5.5745
5	2	2	3	1	-6.0365	-6.0713	-0.58	-6.0365	-6.0944	-6.0365
6	2	3	1	2	-5.4919	-5.4803	0.21	-5.4919	-5.5035	-5.4456
7	3	1	3	2	-6.2247	-6.2131	0.19	-6.2247	-6.2363	-6.1784
8	3	2	1	3	-5.9035	-5.8803	0.39	-5.9035	-5.9035	-5.8456
9	3	3	2	1	-5.7893	-5.824	-0.60	-5.7893	-5.8472	-5.7893

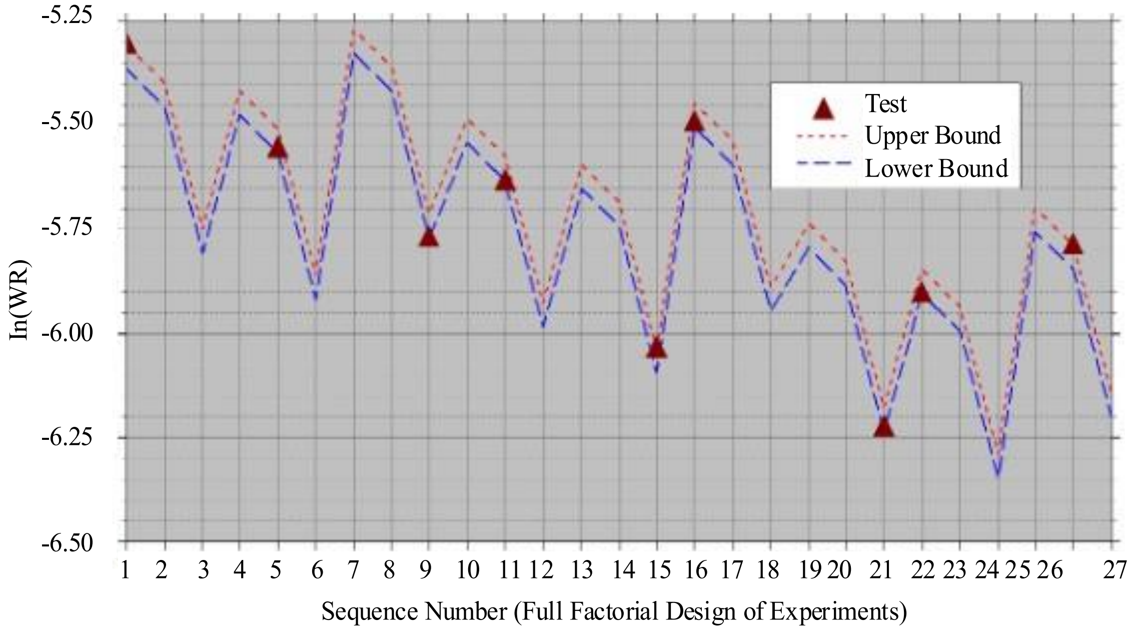

Figure 2. Comparison of $\ln WR$ between Test data [24] and estimates

To demonstrate the effectiveness of the Eq. (3), the set of parameters (*A*=0, *B*=1, *C*=1000) to the Test Run-1 is considered. The coded values to this set of parameters are $(\xi_1 = -1, \xi_2 = -1, \xi_3 = -1)$. Using them in Eq. (3) results

$$\ln WR = -5.7197 - 0.21445 \times (-1) - 0.03775 \times (-1)^2 + 0.0187 \times (-1) + 0.1291 \times (-1)^2$$
$$- 0.2216 \times (-1) - 0.1301 \times (-1)^2$$
$$= -5.7197 + 0.21445 - 0.03775 - 0.0187 + 0.1291 + 0.2216 + 0.1301 \approx -5.3411$$

Journal of Polymer & Composites
Volume 14, Special Issue 1
ISSN: 2321-2810 (Online), ISSN: 2321-8525 (Print)

Applying corrections -0.0232 and 0.0347, lower and upper bound values of $\ln WR$ obtained are -5.3643 and -5.3064, which are in good agreement with those in Table 5. Figure 3 shows a good comparison of $\ln WR$ estimates using equations (2) and (3) for the full factorial design of experiments, which confirms the validity of the developed empirical relationship (3).

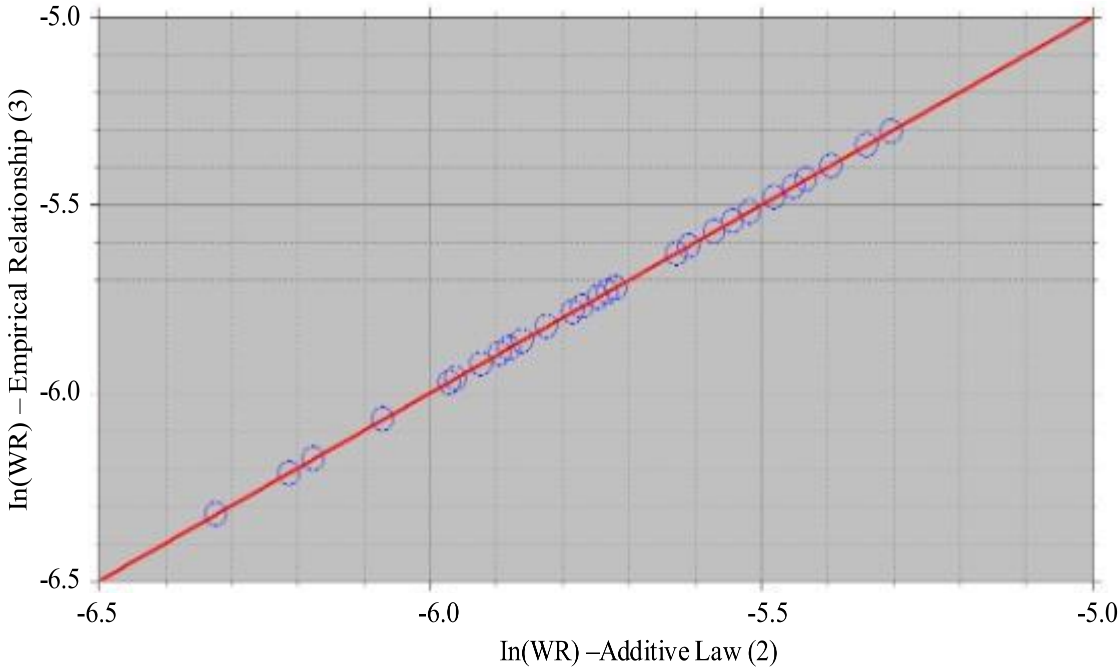

Figure 3. Comparison of $\ln WR$ estimates from (2) and (3)

RESULTS AND DISCUSSION

Experimental results in the preceding section were based on the Taguchi's L_9 OA to examine the dry sliding wear characteristics of stir-cast AA7050/SiC metal matrix composite. ANOVA performed to assess the influence of the process variables on the wear rate. By examining ANOVA Table 4, it is possible to determine a set of process parameters $A_3\,B_2\,C_3$ (with subscripts indicating the respective levels of parameters) that result in the minimum $\ln WR$ value. The optimal process parameters to yield the minimum $\ln WR$ value are: SiC reinforcement, A_3=6%; sliding velocity, B_2=2 m/s; and sliding distance, C_3=1800 m. The minimum $\ln WR$ value estimated from the additive law (2) is -6.3235 and from the empirical relationship (3) is -6.3236. The range of $\ln WR$ estimate is from -6.3467 to -6.2888. Hence, the range of wear rate, $WR\,(= \exp(\ln WR))$ estimate is from 0.00175 to 0.00186 mm^3/m. Table 6 presents the wear rate (WR), for the 27 combinations of the three process parameters and three levels using the additive law (2) and the developed empirical relationship (3). The measured *WR* values in Table 6 are within the estimated range.

To visually underscore the attainment of the low wear rate, *WR* curves in Figures 4 to 6 were generated using the empirical relationship (3), specifically by fixing two process variables at their optimal values, while progressively varying the third. For the sliding velocity, B_2=2 m/s and sliding distance, C_3= 1800 m, the wear rate (*WR*) in Figure 4 decreases with % of SiC reinforcement (*A*). For the SiC reinforcement, A_3= 6%, and sliding distance, C_3=1800 m, *WR* decreases with sliding velocity (*B*) in Figure 5 up to 2 m/s and later on increases up to 3 m/s. For the SiC reinforcement, A_3= 6%, and sliding velocity, B_2=2 m/s, *WR* decreases with sliding distance (*C*) in Figure 6. Figures 4 to 6 demonstrate the low value of *WR* at the identified optimal processing conditions.

Table 6. Comparison of measured and estimates of *WR*.

S. No.	Levels of Process Parameters			Wear Rate, *WR* (mm^3/m)				
				Test [24]	*Additive law (2) Expected range*		*Empirical relation (3) Expected range*	
	A	*B*	*C*		*From*	*To*	*From*	*To*
1	1	1	1	0.00496	0.00468	0.00496	0.00468	0.00496
2	1	1	2		0.00427	0.00453	0.00427	0.00453
3	1	1	3		0.00301	0.00318	0.00301	0.00318
4	1	2	1		0.00419	0.00444	0.00419	0.00444
5	1	2	2	0.00387	0.00383	0.00405	0.00383	0.00405
6	1	2	3		0.00269	0.00285	0.00269	0.00285
7	1	3	1		0.00486	0.00515	0.00486	0.00515
8	1	3	2		0.00443	0.00470	0.00443	0.0047
9	1	3	3	0.00312	0.00312	0.00331	0.00312	0.00331
10	2	1	1		0.00392	0.00416	0.00392	0.00416
11	2	1	2	0.00358	0.00358	0.00379	0.00358	0.00379
12	2	1	3		0.00252	0.00267	0.00252	0.00267
13	2	2	1		0.00351	0.00372	0.00351	0.00372
14	2	2	2		0.00321	0.00340	0.00321	0.0034
15	2	2	3	0.00239	0.00226	0.00239	0.00226	0.00239
16	2	3	1	0.00412	0.00407	0.00432	0.00407	0.00432
17	2	3	2		0.00372	0.00394	0.00372	0.00394
18	2	3	3		0.00261	0.00277	0.00261	0.00277
19	3	1	1		0.00305	0.00323	0.00305	0.00323
20	3	1	2		0.00278	0.00295	0.00278	0.00295
21	3	1	3	0.00198	0.00196	0.00207	0.00196	0.00207
22	3	2	1	0.00273	0.00273	0.00289	0.00273	0.00289
23	3	2	2		0.00249	0.00264	0.00249	0.00264
24	3	2	3		0.00175	0.00186	0.00175	0.00186
25	3	3	1		0.00316	0.00335	0.00316	0.00335
26	3	3	2	0.00306	0.00289	0.00306	0.00289	0.00306
27	3	3	3		0.00203	0.00215	0.00203	0.00215

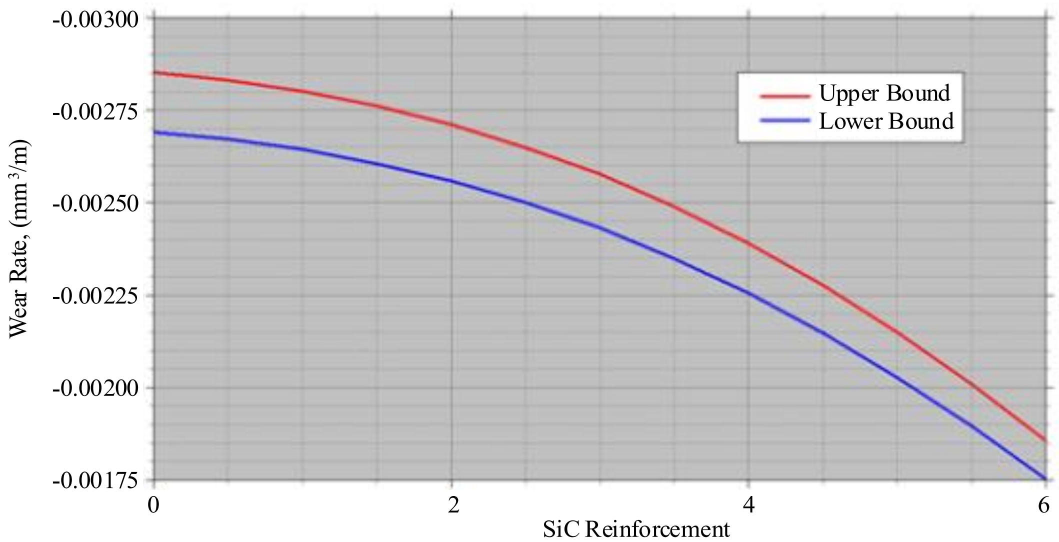

Figure 4. Wear rate (*WR*) versus reinforcement (*A*) showing low value of *WR* at A_3= 6% for the specified sliding velocity, B_2=2 m/s and sliding distance, C_3=1800 m.

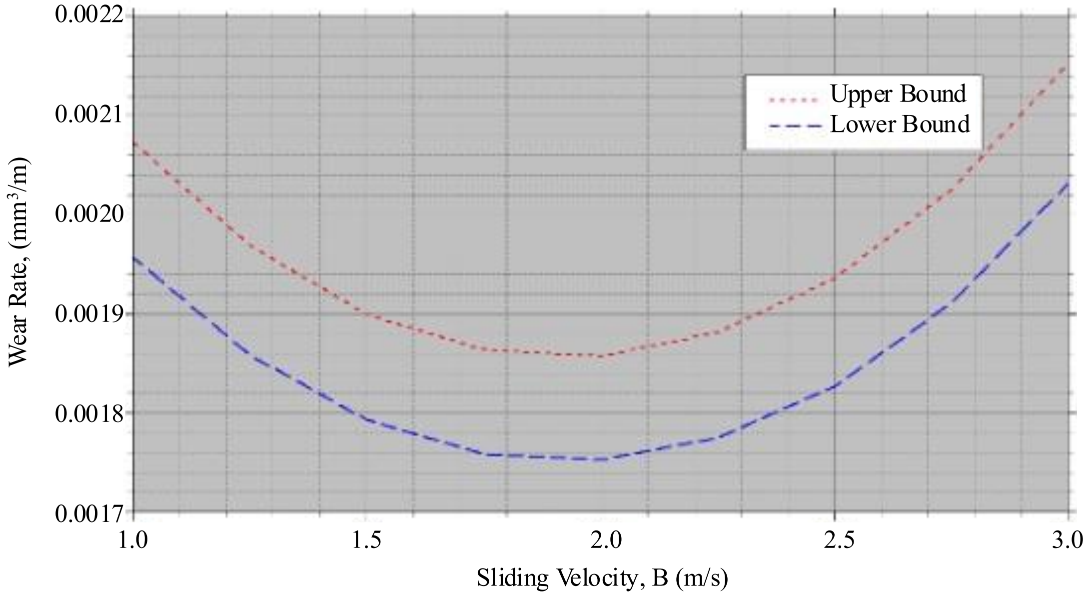

Figure 5. Wear rate (*WR*) versus sliding velocity (*B*) showing low value of *WR* at B_2=2 m/s for the specified reinforcement, A_3=6%, and sliding distance, C_3=1800 m

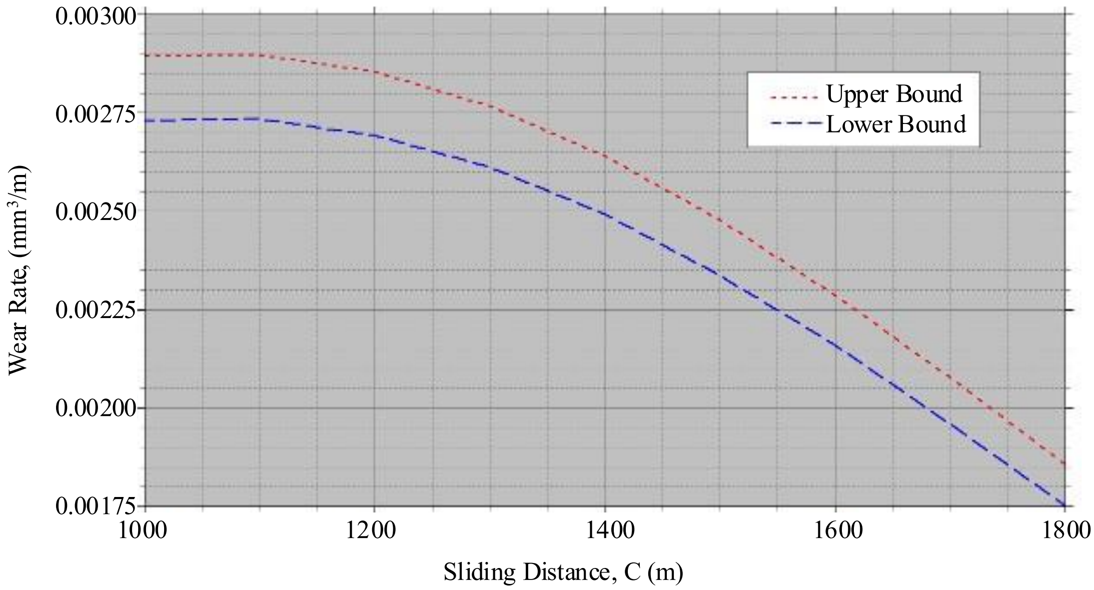

Figure 6. Wear rate (*WR*) versus sliding distance (*C*) showing low value of WR at C_3= 1800 m for the specified reinforcement, A_3= 6% kg, and sliding velocity, B_2=2 m/s.

CONCLUSION

This investigation focused on understanding the dry sliding wear characteristics of an AA7050/SiC metal matrix composite, which was produced using a stir-casting technique. The experimental design and subsequent analysis were carried out with the aid of a pin-on-disc tribometer. The composite's fabrication process involved melting the AA7050 alloy, carefully introducing silicon carbide (SiC) particles, stirring to achieve homogeneous dispersion, and finally, casting the molten mixture.

To evaluate the wear rate (*WR*), individual test specimens, precisely 35 mm in length and 9 mm in diameter, were subjected to testing. The wear rate was assessed as a function of three operational variables, each assigned at three relevant levels for tribological applications: the percentage of reinforcement, the sliding velocity, and the total sliding distance. To systematically identify optimal conditions, Taguchi's L_9 orthogonal array was employed, defining nine distinct experimental configurations. Following the tests, a statistical analysis was performed to quantify the individual percentage contribution of each parameter to the observed wear rate.

To account for the significant variation observed in the wear rate (*WR*) measurements recorded over the nine test runs in the Taguchi's L_9 OA, the dependent variable (*WR*) data is transformed to a natural logarithmic scaling. This resulting statistically adjusted metric is formally designated as $\ln WR$. The analysis revealed that both the reinforcement percentage and the sliding distance exerted a dominant influence on the grand mean value of $\ln WR$, contributing 43.01% and 50.66% respectively. In contrast, the sliding velocity played a comparatively minor role, accounting for only 5.46% of the overall mean $\ln WR$. An empirical model correlating the wear rate with these operational parameters was successfully developed and subsequently validated against the experimentally acquired data. The study successfully identified the optimal set of operational parameters as: 6% reinforcement, a sliding velocity of 2 m/s, and a total sliding distance of 1800 m. Through the modified Taguchi methodology, the minimum anticipated wear rate was estimated to fall within the narrow range of 0.00175 to 0.00186 mm^3/m. The AA7050/SiC metal matrix composite thus demonstrates superior resistance to surface degradation due to reinforcement of the SiC particles. However, the optimal variables (parameters) in this study are applicable to the existing experimental design dimensions and materials, not a generic one. Given the existing body of knowledge concerning the manufacturing processes for this MMC and the established data regarding its resistance to wear, the primary goal for prospective research is the systematic refinement of the composite's functional qualities. This optimization effort is focused on the comprehensive study of how adjustments to the geometry (size and form) and the spatial alignment (distribution) of the SiC reinforcement phase impact performance, alongside the evaluation of pioneering synthesis and fabrication methodologies.

REFERENCES

1. Arwin R, Abraham S, Rajendran P, Prakash Shanmugasundaram R. Reinforcement of SiCParticles on Friction Stir Processing of Aluminium AA7050. Engineering Proceedings. 2024 Feb 16;61(1):45.
2. Kumar N, Maheshwari S. Expounding the influence of micro/nano particles on mechanical and tribological properties of AA 7050 matrix composite: a review. Materials Today: Proceedings. 2022 Jan 1;62:3361-7.
3. Vijumon VT, Moses JT, Aloysius PJ, Muthu MN. Development of Novel Wear Equation of AA7050/SiC-Steel Interface for High Temperature Application. Materials Science. 2024 Feb 20;30(1):34-9.
4. Veerandra P, Deepak M. Evaluation of Mechanical Properties and Micro Structural study of AA 7050 Reinforced with SiC Metal Matrix Composite. Int J Res. 2019;6(13):514-30.
5. Gök DA, Bayraktar C, Hoşkun M. A review on processing, mechanical and wear properties of Al matrix composites reinforced with Al2O3, SiC, B4C and MgO by powder metallurgy method. Journal of Materials Research and Technology. 2024 Jul 1;31:1132-50.
6. Gupta PK, Trivedi AK, Gupta MK, Dixit M. Metal matrix composites for sustainable products: A review on current development. Proceedings of the Institution of Mechanical Engineers, Part L: Journal of Materials: Design and Applications. 2024 Oct;238(10):1827-64.
7. Islam MS, Shahruzzaman M, Khan MN, Islam MM, Kabir SF, Mallik AK, Rahman MM, Haque P. Composite materials: Concept, recent advancements, and applications. InRenewable polymers and polymer-metal oxide composites 2022 Jan 1 (pp. 1-43). Elsevier.
8. Chakravarty S, Haldar P, Nandi T, Sutradhar G. Enhancement of mechanical properties and machinability of aluminium composites by cupola slag reinforcements. Materialwissenschaft und Werkstofftechnik. 2024 Sep;55(9):1250-67.

ISSN: 2321-2810 (Online), ISSN: 2321-8525 (Print)

9. Anijdan SM, Sabzi M. The effect of pouring temperature and surface angle of vortex casting on microstructural changes and mechanical properties of 7050Al-3 wt% SiC composite. Materials Science and Engineering: A. 2018 Nov 8;737:230-5.
10. Sankar T, Mohanavel V. Investigations on the mechanical and corrosion properties of silicon nitride reinforced AZ61 composites. Materials Today: Proceedings. 2024 Jul 15.
11. Subha S, Benny N, Singh D. Thermo-mechanical behavior of SiC-based composites for gas turbine engines. Materials Today: Proceedings. 2022 Jan 1;68:2301-9.
12. Mosisili M, Msomi V, Mabuwa S. SiC, titanium, nickel, and ferric acid reinforcement materials to enhance mechanical properties in aluminium alloys: A critical review. Materials Today: Proceedings. 2022 Jan 1;56:2268-73.
13. Khodabakhshi F, Gerlich AP, Švec P. Fabrication of a high strength ultra-fine grained Al-Mg-SiC nanocomposite by multi-step friction-stir processing. Materials Science and Engineering: A. 2017 Jun 20;698:313-25.
14. Senthil Kumar BR, Gopalarama Subramaniyan G, Pragadish N, Venkatesh PM, Sanjay S, Velu CM, Navaneethakrishnan G, Vellingiri S, Govindarajan V. Investigations on wear behavior of aluminium composites at elevated temperature. Advances in Materials Science and Engineering. 2022;2022(1):9594798.
15. Kumar A, Kumar R, Kumar A. Study of wear rate of AA7050-7.5 B4C-T6 composite and optimization of response parameters using taguchi analysis. Int J Exp Res Rev. 2024;39:73-81.
16. Garg HK, Sharma S, Kumar R, Manna A, Dwivedi SP, Abbas M, Kumar A, Khan MI, Bisht YS. Mechanical, tribological, and morphological properties of SiC and Gr reinforced Al-0.7 Fe-0.6 Si-0.375 Cr-0.25 Zn based stir-casted hybrid metal matrix composites for automotive applications: Fabrication and characterizations. Journal of Materials Research and Technology. 2024 Jan 1;28:3267-85.
17. Sakthivelu S, Meignanamoorthy M, Ravichandran M, Sethusundaram PP. Tribological Behavior of AA7050-ZrSiO 4 Composites Synthesized by Stir Casting Technique. Mechanics & Mechanical Engineering. 2019 Jan 1;23(1).
18. de Rojas Candela CS, Riquelme A, Rodrigo P, Torres B, Rams J. Wear behavior of additively manufactured 316L/SiCp composites with up to 60 wt% SiCp. Ceramics International. 2022 Nov 15;48(22):33736-50.
19. Chourasiya A, Krishna CM. Mechanical and microstructure behavior of AA7050 metal matrix composite reinforced with TiO2/BN. International Journal of Metalcasting. 2024 Oct;18(4):3248-62.
20. Venkatesan S, Xavior MA. Tensile behavior of aluminum alloy (AA7050) metal matrix composite reinforced with graphene fabricated by stir and squeeze cast processes. Science and technology of materials. 2018 May 1;30(2):74-85.
21. Yang B, Wu M, Li X, Zhang J, Wang H. Effects of cold working and corrosion on fatigue properties and fracture behaviors of precipitate strengthened Cu-Ni-Si alloy. International Journal of Fatigue. 2018 Nov 1;116:118-27.
22. Ranganathan A, Krishnan PA, Nambiar AS, Kumar SM, Kumar VR. Mechanical characterization of AA7050-TiC metal matrix composites under as cast as condition. Materials Today: Proceedings. 2018 Jan 1;5(11):25368-75.
23. Jagatheeshwaran MS, Elayaperumal A, Arulvel S. The role of calcinated sea shell particles on friction-wear behavior of electroless NiP coating: fabrication and characterization. Surface and Coatings Technology. 2016 Oct 25;304:492-501.
24. Sathish T, Karthick S. Wear behaviour analysis on aluminium alloy 7050 with reinforced SiC through taguchi approach. Journal of Materials Research and Technology. 2020 May 1;9(3):3481-7.
25. Ross PJ. Taguchi techniques for quality engineering: loss function, orthogonal experiments, parameter and tolerance design.
26. Sanjay Krishna GR, Sai Sarath K, Nageswara Rao B, Atgur V, Banapurmath NR, Vadlamudi C, Krishnappa S, Umarfarooq MA, Sajjan AM. Specification of the optimal gas metal arc welding

(GMAW) parameters to enhance the mild steel strength (MS1018). Materials Express. 2023 Dec 1;13(12):2137-44.

27. Anantha MT, Pyatla S, Koneru S, Reddy KP, Boggarapu NR. Optimal turning process parameters for finer surface finish of AZ31 Mg alloy rods for automotive products. International Journal of Vehicle Structures & Systems. 2024 Apr 1;16(2):156-60.

